Article

Remote Sensing and Soil Moisture Sensors for Irrigation Management in Avocado Orchards: A Practical Approach for Water Stress Assessment in Remote Agricultural Areas

Emmanuel Torres-Quezada [1], Fernando Fuentes-Peñailillo [2,3,*], Karen Gutter [4], Félix Rondón [5], Jorge Mancebo Marmolejos [5], Willy Maurer [5] and Arturo Bisono [6]

1 Horticultural Science Department, North Carolina State University, 2721 Founders Dr., Raleigh, NC 27607, USA; eatorre3@ncsu.edu
2 Vicerrectoría Académica, Universidad de Talca, Talca 3460000, Chile
3 Centro de Sistemas de Ingeniería KIPUS, Universidad de Talca, Curicó 3340000, Chile
4 Doctorado en Ciencias Agrarias, Facultad de Ciencias Agrarias, Universidad de Talca, Talca 3460000, Chile; kgutter@utalca.cl
5 Department of Agronomy, Specialized Institute of Higher Studies Loyola, San Cristóbal 91000, Dominican Republic; frondon@ipl.edu.do (F.R.); jmancebo@ipl.edu.do (J.M.M.); wmaurer@ipl.edu.do (W.M.)
6 Universidad Tecnológica de Santiago (UTESA), Av. Salvador Estrella Sadhalá esq, Santiago de los Caballeros 51000, Dominican Republic; abisono@utesa.edu
* Correspondence: ffuentesp@utalca.cl

Abstract: Water scarcity significantly challenges agricultural systems worldwide, especially in tropical areas such as the Dominican Republic. This study explores integrating satellite-based remote sensing technologies and field-based soil moisture sensors to assess water stress and optimize irrigation management in avocado orchards in Puerto Escondido, Dominican Republic. Using multispectral imagery from the Landsat 8 and 9 satellites, key vegetation indices (NDVI and SAVI) and NDWI, a water-related index that specifically indicates changes in crop water contents, rather than vegetation vigor, were derived to monitor vegetation health, growth stages, and soil water contents. Crop coefficient (Kc) values were calculated from these vegetation indices and combined with reference evapotranspiration (ETo) estimates derived from three meteorological models (Hargreaves–Samani, Priestley–Taylor, and Blaney–Criddle) to assess crop water requirements. The results revealed that soil moisture data from sensors at 30 cm depth strongly correlated with satellite-derived estimates, reflecting avocado trees' critical root zone dynamics. Additionally, seasonal patterns in the vegetation indices showed that NDVI and SAVI effectively tracked vegetative growth stages, while NDWI indicated changes in the canopy water content, particularly during periods of water stress. Integrating these satellite-derived indices with field measurements allowed a comprehensive assessment of crop water requirements and stress, providing valuable insights for improving irrigation practices. Finally, this study demonstrates the potential of remote sensing technologies for large-scale water stress assessment, offering a scalable and cost-effective solution for optimizing irrigation practices in water-limited regions. These findings advance precision agriculture, especially in tropical environments, and provide a foundation for future research aimed at enhancing data accuracy and optimizing water management practices.

Keywords: biosystem engineering; crop water stress; satellite data; agricultural sustainability; precision agriculture

1. Introduction

Water scarcity is one of the most pressing challenges in modern agriculture, exacerbated by climate change and the increasing demand for fresh water for urban areas [1,2]. Irrigated agriculture, which accounts for approximately 70% of global freshwater use, faces significant challenges in water management [3,4]. However, to properly assess these challenges, it is necessary to consider each country's geographical and socioeconomic differences and generate water management strategies specific to each location.

In this sense, countries such as the Dominican Republic are characterized by substantial regional climatic differences in seasonal and annual rainfall, with temperature variations primarily defined by altitude. This indicates a significant climatic heterogeneity influenced by geographical features and marine conditions [5,6]. Because of this, the Dominican Republic has a diverse agricultural sector that cultivates key crops such as mango, cocoa beans, bananas, tobacco, and avocado [7]. The latter is a widely grown crop, especially in regions with tropical and subtropical climates, and has reached great relevance worldwide because of its health benefits and culinary versatility [8]. However, avocado trees are also characterized by having high water demands and vulnerability to water stress, which can negatively affect crop yields, quality, and sustainability [9,10]. Therefore, in the context of the high global demand for avocados, it is essential to maintain optimal fruit quality to ensure that small and medium producers are competitive [11] while also considering the current water scarcity scenario.

Regarding irrigation management, it is essential to consider that the avocado roots that allow nutrient and water uptake correspond to the fine roots in the top 30 cm of the soil [12]. Therefore, irrigation methods such as drip irrigation, which provides precise water application directly to the root zone, and overhead sprinkling, which can cover larger areas but may lead to water loss through evaporation [8,12], must focus on this specific area of the root zone. Different technologies are currently being used in field settings to assess irrigation delivery effectiveness, which can sometimes be managed remotely to provide valuable insights into how much water to apply and when. This often involves soil moisture sensors that provide real-time or historical data and control automated systems. These tools can also be compared to remote sensing technologies such as satellite images, given that in regions where conventional irrigation management practices are not feasible due to technological constraints, remote sensing technologies offer a promising alternative for monitoring water stress and optimizing irrigation practices [13–15].

Satellite remote sensing has emerged as a valuable tool in agricultural water management, providing global coverage at a relatively high spatial resolution and monitoring vegetation health and water status over large areas [16–18]. Vegetation indices derived from satellite imagery, such as the Normalized Difference Vegetation Index (NDVI), Soil-Adjusted Vegetation Index (SAVI), and Normalized Difference Water Index (NDWI), have been widely used to estimate vegetation vigor and stress [19,20]. The NDVI, based on the differential reflectance of red and near-infrared light, is particularly useful for assessing plant health and monitoring crop water stress, making it an essential tool in precision agriculture [21–23]. In contrast, the SAVI and NDWI are well suited to estimating the vigor of vegetation cover and its growth dynamics [24,25].

While satellite imagery has proven effective for vegetation monitoring, its integration with ground-based measurements is critical for enhancing the accuracy and reliability of water stress assessments. Soil moisture, a key indicator of plant water availability, is often measured at various depths to understand root-zone water content dynamics [26–28]. However, obtaining accurate soil moisture data in remote agricultural areas can take time due to logistical and financial constraints. The European Centre for Medium-Range Weather Forecasts (ECMWF) provides global soil moisture estimates through the ERA-5 dataset,

which offers hourly soil moisture data at different depths, facilitating the assessment of soil water contents across large areas. However, validating these remote sensing data with ground measurements is necessary to ensure their reliability.

Field-based sensors can measure soil moisture at multiple depths (e.g., 10 cm, 30 cm, and 60 cm) and validate the remotely sensed soil moisture data in this context. These sensors enable an accurate understanding of soil moisture dynamics, particularly in regions where advanced irrigation practices still need to be fully implemented and where large-scale monitoring infrastructure is limited.

Along with soil moisture measurements, crop water stress is influenced by evapotranspiration, which refers to the combined process of water evaporation from the soil and plant transpiration. ET is a key component in irrigation management, as it reflects the water lost from the production system and helps estimate crop water needs. The FAO Penman–Monteith equation is widely regarded as the most reliable method for calculating the reference evapotranspiration (ETo). Still, alternative strategies, such as the Hargreaves–Samani and Priestley–Taylor models, are also commonly used, particularly in areas where meteorological data are sparse [29,30].

While these models differ in their approach, they are all helpful in estimating ETo and understanding crop water requirements. To address all the abovementioned limitations, this study seeks to integrate satellite remote sensing technologies and field-based soil moisture sensors to assess water stress and optimize irrigation practices in avocado orchards in a tropical agricultural environment. By combining vegetation indices derived from multispectral imagery with soil moisture data collected at critical depths, this study aims to comprehensively understand water dynamics and crop stress. This is done by focusing on (i) vegetation monitoring through the use of indices such as the NDVI, SAVI, and NDWI to capture vegetation health, growth stages, and canopy water contents; (ii) soil moisture assessment by deploying sensors at varying depths to monitor the soil water content within the critical root zone and validate remotely sensed data; and (iii) irrigation optimization by estimating crop water requirements using reference evapotranspiration models and crop coefficients derived from vegetation indices.

Our goal is to demonstrate how remote sensing, combined with ground-based soil moisture sensors and evapotranspiration models, can offer an innovative and practical solution for optimizing irrigation practices. The outcomes of this study will contribute to improving irrigation strategies in avocado orchards and provide insights that can be applied to other crops in water-scarce regions, thereby supporting sustainable agricultural practices worldwide.

2. Materials and Methods

2.1. Study Area

This study was conducted in an avocado (*Persea americana*) orchard in Puerto Escondido (18.340°N, 71.605°W, 447 m.a.s.l.) (Figure 1), Dominican Republic, during the 2021 and 2022 growing seasons, covering an area of 3.58 hectares. This location is characteristic of the region's small- to medium-scale agricultural systems. The climate of Puerto Escondido is subtropical, with distinct wet and dry seasons. The annual temperature ranges from 23 °C to 31 °C. The rainy season lasts from May to October, contributing to most of the annual rainfall, while the dry season (November to April) presents irrigation challenges due to limited water resources. The topography is moderately undulating, with slight slopes influencing water infiltration and drainage. The soil is primarily loamy, with good water retention capacity but localized texture and moisture variability due to microclimatic differences. This site was selected as a representation of a water-limited agricultural system typical of the region and was well suited for collecting satellite and field data.
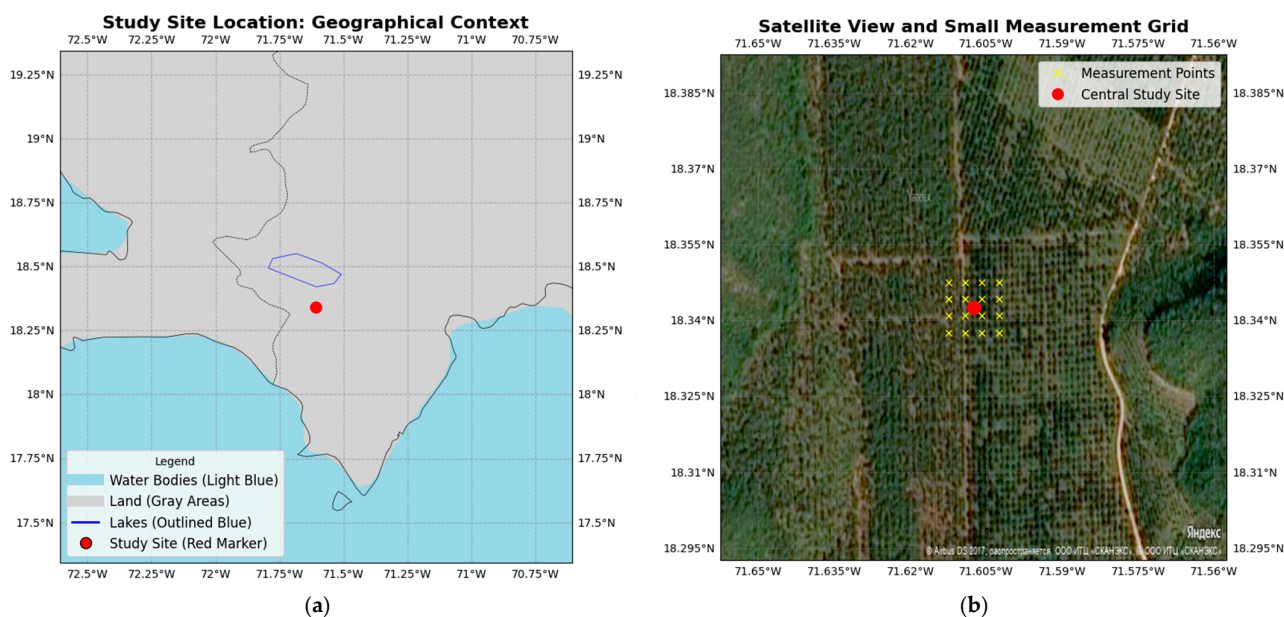
Figure 1. (**a**) The geographical location of the study site; (**b**) a high-resolution satellite image of the orchard. Both maps include latitude and longitude references in degrees (WGS 84/EPSG:4326) to ensure spatial accuracy.

2.2. Data Collection

2.2.1. Satellite Data

The seasonal vegetation health and water status dynamics were analyzed using the NDVI, SAVI, and NDWI derived from Landsat 8 and 9 satellite imagery collected during the 2021 and 2022 growing seasons. Given the 30 m spatial resolution of Landsat 8 and 9, each pixel may contain a mixture of avocado canopy, bare soil, and surrounding vegetation. To address this, we focused on homogeneous orchard blocks and computed the standard deviation of the vegetation indices to assess the pixel variability. This approach allowed us to estimate the pixel heterogeneity and minimize potential biases.

The trends in these indices were analyzed in conjunction with soil moisture data and local climatic conditions to provide a comprehensive understanding of crop responses to water stress across the orchard. By focusing on uniform orchard blocks, we ensured consistency between the satellite data and field conditions. This ensured that the indices were representative of the entire orchard, minimizing the impact of heterogeneous areas.

It is important to note that Landsat 8 and 9 imageries were exclusively used to derive the vegetation indices (NDVI, SAVI, NDWI) for monitoring crop health and water status. Soil moisture estimates from in situ sensors and ERA5 reanalysis data provided complementary ground-truth information. To mitigate the limitations of Landsat's 30 m resolution, we focused on uniform orchard blocks and complemented the satellite data with field measurements. For each index, satellite-derived values were interpolated to daily measurements to track temporal variability. The standard deviations of these values were calculated to assess spatial variability within the study area, highlighting heterogeneous vegetation responses to environmental conditions. The daily vegetation index values and their standard deviations were graphed to illustrate the temporal dynamics and variability of vegetation health and water availability across the growing seasons.

The NDVI, a primary index for vegetation vigor and chlorophyll content, was calculated using the following formula [31,32]:

$$NDVI = \frac{NIR - Red}{NIR + Red} \tag{1}$$

where NIR and Red represent near-infrared and red reflectance values, respectively. High NDVI values indicate dense and healthy vegetation.

To account for soil reflectance, particularly in areas with partial canopy cover, the Soil-Adjusted Vegetation Index (SAVI) was employed [33,34]. The SAVI is calculated as follows:

$$\text{SAVI} = \frac{(\text{NIR} - \text{Red})(1 + \text{L})}{\text{NIR} + \text{Red} + \text{L}} \tag{2}$$

where L is a correction factor set to 0.5 for intermediate canopy cover conditions. This adjustment improves the accuracy of vegetation monitoring in heterogeneous landscapes.

The Normalized Difference Water Index (NDWI) was calculated to estimate the canopy water content using the following formula [35,36]:

$$\text{NDWI} = \frac{\text{Green} - \text{NIR}}{\text{Green} + \text{NIR}} \tag{3}$$

where Green and NIR represent green and near-infrared reflectance values, respectively. The NDWI is highly sensitive to the water content within the canopy and offers insights into plant water status.

Figure 2 illustrates the spectral coverage and complementarity of the relevant Landsat 8 and Landsat 9 bands, highlighting the bands used to calculate the NDVI, SAVI, and NDWI, with their corresponding wavelength ranges. The satellite imagery was preprocessed using the Google Earth Engine (GEE) platform to ensure data reliability and consistency. This preprocessing involved cloud masking, radiometric calibration, and atmospheric corrections. Cloud masking was applied using the Landsat surface reflectance QA band to exclude pixels affected by clouds and shadows. Radiometric calibration standardized the data across the acquisition dates, converting digital numbers into surface reflectance values. Atmospheric corrections were applied to account for the effects of aerosols and water vapor, improving the accuracy of the spectral bands used for the vegetation indices.
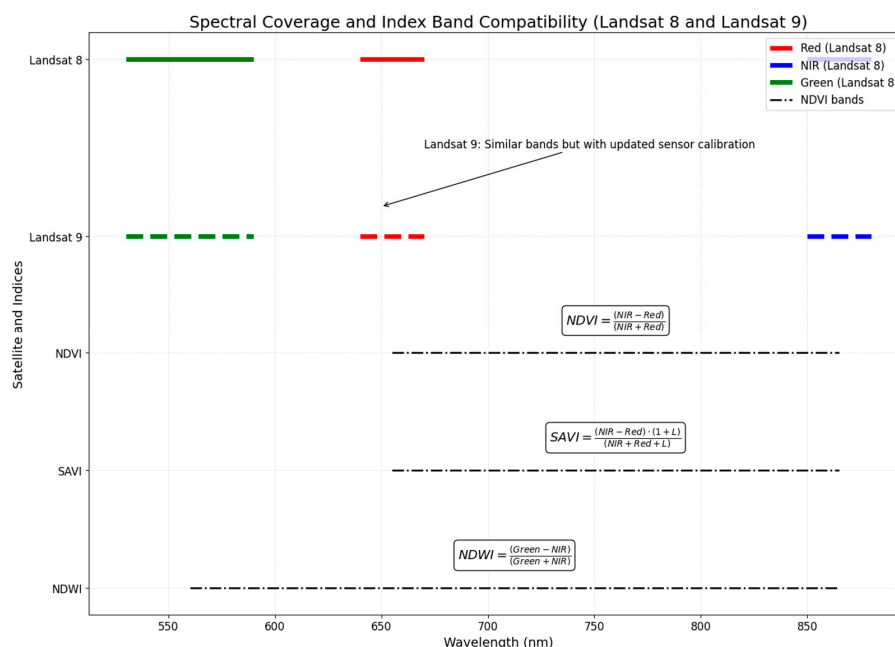

Figure 2. Spectral reflectance curves of avocado orchards derived from Landsat 8 and 9 satellite data. The figure shows the distinct spectral bands (blue, green, red, near-infrared, and shortwave infrared) used to calculate the vegetation and water indices. The variation in reflectance values across these bands provides insights into plant health, water contents, and stress conditions. Seasonal changes in reflectance highlight the impact of varying water availability on vegetation indices, illustrating how water stress influences plant vitality throughout the growing season.

For the analysis, the vegetation indices were computed for each satellite image, and seasonal trends were analyzed through temporal aggregation methods, including calculating seasonal averages and identifying peaks in the indices. This approach, used in several studies [37–42], helped assess changes in vegetation health and water stress throughout the growing seasons.

Additionally, soil moisture estimates from ERA5, provided by the European Centre for Medium-Range Weather Forecasts (ECMWF) through the Copernicus Climate Data Store, were integrated into the analysis. ERA5 provides hourly soil moisture data with global coverage, providing a consistent perspective on soil water dynamics. These estimates were aggregated to match the temporal resolution of the satellite imagery, enabling the validation and contextualization of the remotely sensed soil moisture data.

2.2.2. Sensor Data for Soil Moisture and Climate Monitoring

To validate satellite-derived soil moisture data from ERA5 against in situ field measurements collected at various depths within the avocado orchard, the soil moisture was measured using Watermark sensors installed at depths of 30 cm, 60 cm, and 120 cm along the planting beds in representative locations within the avocado orchard. The soil moisture sensors were strategically deployed across representative orchard blocks, with each sensor coded according to its location and depth. The sensor naming convention included a block identifier (e.g., "A", "B") and depth indicators (e.g., "S1-30" for a 30 cm depth sensor) representing the three soil depth categories: 30 cm, 60 cm, and 120 cm (Figure 3). This deployment design enabled comprehensive soil moisture monitoring at both horizontal and vertical scales, which is crucial for evaluating the spatial and temporal accuracy of satellite-derived moisture estimates.
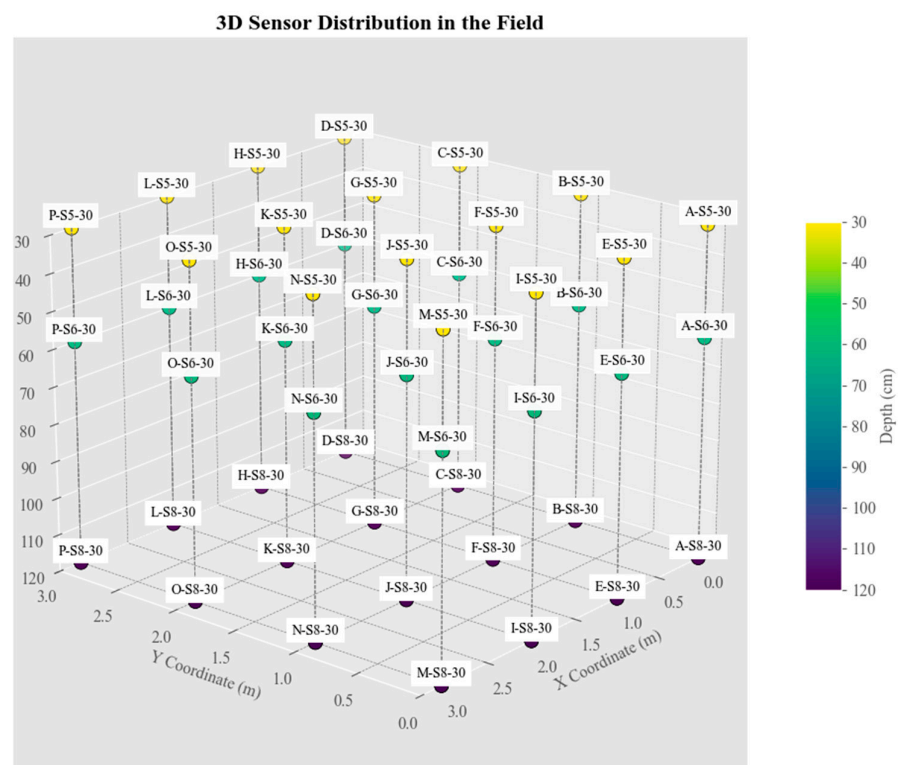
Figure 3. Three-dimensional spatial distribution of sensors in the field. The horizontal plane (X and Y coordinates) represents the layout of the field, where the distances in meters are illustrative and do not reflect the actual distance between sensors. In contrast, the vertical axis (Z coordinate) corresponds to the sensor placement depth in centimeters.

These sensors were installed during the study period. Raw field sensor readings were recorded in centibars and converted to volumetric soil moisture contents (m^3/m^3) to ensure comparability with satellite data. This conversion was based on a calibration table that linked tension values to soil-specific moisture states, including the field capacity (FC) and permanent wilting point (PWP). These transformations provided a consistent framework for comparing field and satellite data, strengthening the analysis.

Pearson correlation coefficients (r) and *p*-values were calculated to evaluate the agreement between the field measurements and ERA5 soil moisture estimates, quantifying the accuracy of the satellite data. These calculations were performed separately for each sensor, grouped by depth and growing season (2021 and 2022). The resulting correlations provided valuable insights into the performance of the field sensors and satellite estimates, allowing for a clear understanding of the spatial variability and the temporal dynamics of soil moisture. Seasonal analyses were conducted yearly to evaluate the interannual variability in the correlation results.

Meteorological data were collected using an agro-meteorological station operated by a local commercial entity adjacent to the orchard. The station provided high-resolution hourly recordings of air temperature (°C), relative humidity (%), and solar radiation (MJ/m^2). These air temperature data were critical for understanding the thermal conditions affecting evapotranspiration rates and crop physiological responses. Relative humidity measurements enabled the calculation of the vapor pressure deficit (VPD), a key indicator of atmospheric water demand, using saturation and actual vapor pressures derived from recorded temperature and humidity values. Solar radiation data quantified the incoming energy available for evapotranspiration and photosynthesis, while the VPD provided a comprehensive measure of the atmospheric potential to induce plant water stress. The meteorological data were aggregated into daily averages to match the temporal resolution of the satellite data. These aggregated datasets were aligned with the soil moisture and vegetation index data, ensuring temporal consistency for integrated analyses.

The meteorological station was strategically located adjacent to the study orchard to capture representative environmental data influencing the crop's water dynamics. While microclimatic variations may exist due to differences in vegetation cover or terrain within the orchard, previous observational studies and field measurements indicated relatively uniform conditions across the orchard blocks. Thus, the data from the station reliably reflect the general trends in temperature, solar radiation, and precipitation affecting the study area. However, we acknowledge that finer-scale variability may influence specific microclimates, which could benefit from the deployment of additional in situ sensors in future studies. The distance between the meteorological station and the orchard was approximately 200 m, ensuring minimal environmental divergence.

2.2.3. Estimation of Crop Water Requirements and Evapotranspiration Models

To estimate the water requirements of the avocado orchard during the 2021 and 2022 growing seasons, crop coefficients (Kc) were derived independently from the NDVI, SAVI, and NDWI. Crop coefficients are dimensionless factors that adjust ETo to reflect the actual water use of the crop (ETc), varying with the crop's growth stage and canopy development, and are able to capture the dynamic water needs throughout the season. The reference evapotranspiration was calculated daily using three meteorological models: the Hargreaves–Samani model, a simplified Priestley–Taylor model, and the Blaney–Criddle model. This framework provided a detailed understanding of crop water dynamics under varying environmental conditions. The crop coefficients were calculated using empirical equations tailored for perennial crops, ensuring relevance to avocado orchards.

The equations for each vegetation index were as follows:

NDVI:

$$Kc = 1.2 \cdot NDVI - 0.15 \tag{4}$$

where 1.2 is a coefficient reflecting the sensitivity of Kc to the NDVI, emphasizing its strong correlation with canopy cover and the leaf area index (LAI), and -0.15 is an intercept that adjusts Kc for sparse vegetation conditions where NDVI values are low.
SAVI:

$$Kc = 1.0 \cdot SAVI - 0.1 \tag{5}$$

where 1.0 is a coefficient capturing the soil-adjusted dynamics of Kc, which is particularly relevant for partial canopy cover conditions, and -0.1 is an intercept to account for soil reflectance under sparse vegetation.
NDWI:

$$Kc = 0.85 \cdot NDWI + 0.05 \tag{6}$$

where 0.85 is a coefficient reflecting the relationship between the canopy water content and Kc, making the NDWI particularly sensitive to changes in water availability, and 0.05 is an intercept ensures that Kc remains positive despite low NDWI values.

The differences in the coefficients and intercepts reflect each vegetation index's unique sensitivities to biophysical characteristics, such as vegetation cover, soil influences, and water contents.

The reference evapotranspiration (ETo) was calculated using three meteorological models chosen for their compatibility with the available meteorological inputs:

Hargreaves–Samani model:

$$ETo = 0.0023 \cdot Rs \cdot (T_{max} - T_{min}) \cdot 0.5 \cdot (T_{avg} + 17.8) \tag{7}$$

where Rs is the solar radiation at the surface (MJ/m^2); T_{max}, T_{min}, and T_{avg} are the maximum, minimum, and average daily temperatures ($^\circ C$); and 0.0023 is a coefficient specific to the Hargreaves–Samani model.
Simplified Priestley–Taylor model:

$$ETo = 0.23 \cdot Rs \tag{8}$$

where 0.23 is a coefficient suited for energy-driven evapotranspiration in humid or energy-limited conditions.
Blaney–Criddle model:

$$ETo = p \cdot (0.46 \cdot T_{avg} + 8) \tag{9}$$

where p is the proportion of annual daytime hours for each day of the year (unitless), T_{avg} is the average daily temperature ($^\circ C$), and 0.46 and 8 are constants derived from the original Blaney–Criddle formulation.

These models were selected to accommodate the available meteorological inputs, which included the daily temperature (T_{max}, T_{min}, T_{avg}), solar radiation (Rs), and estimated daylight hours (p). The derived Kc values for the NDVI, SAVI, and NDWI and the ETo values for each meteorological model were calculated independently. This separation allowed for a robust assessment of each index's relative performance without introducing aggregation biases. By linking vegetation indices to meteorological data, this methodology provides a scalable framework for estimating crop coefficients and reference evapotranspiration in regions with limited meteorological infrastructure, aligning with precision agriculture objectives.

3. Results

3.1. Meteorological Data Analysis

The meteorological data collected during the 2021 and 2022 growing seasons provided essential insights into the environmental conditions influencing the avocado orchard's water dynamics. This analysis focused on key climatic variables recorded at an agro-meteorological station located near the study area, including temperature, precipitation, and solar radiation (Figure 4). The analysis of daily temperature, precipitation, and solar radiation data recorded over the two years revealed significant seasonal trends and fluctuations that directly impacted crop water needs and soil moisture dynamics. The temperature exhibited a clear seasonal pattern, ranging from 23 °C to 31 °C, with the warmest temperatures occurring during the dry season (November to April) and cooler temperatures recorded in the wet season (May to October). Daily temperatures typically reached around 30 °C during the warmest months and dropped to around 15 °C during the cooler periods, reflecting the region's subtropical climate. This temperature variation influenced the ETo rates, contributing to water stress during the warmer months. Precipitation was concentrated during the wet season, with the highest rainfall recorded between May and October. The total annual precipitation in 2021 was approximately 762.2 mm, while in 2022, it was slightly less at 669.03 mm. Despite heavy rain during the wet months, most of the year remained dry, presenting challenges for irrigation management during the dry season. Although significant rainfall spikes were recorded, they were infrequent, resulting in a highly variable distribution of precipitation. Solar radiation followed a consistent seasonal trend, peaking during the dry months and decreasing during the wet season. Higher solar radiation values were observed during the dry season, driven by longer daylight hours and clearer skies; this played a crucial role in photosynthesis and crop transpiration, directly influencing the orchard's water demand.
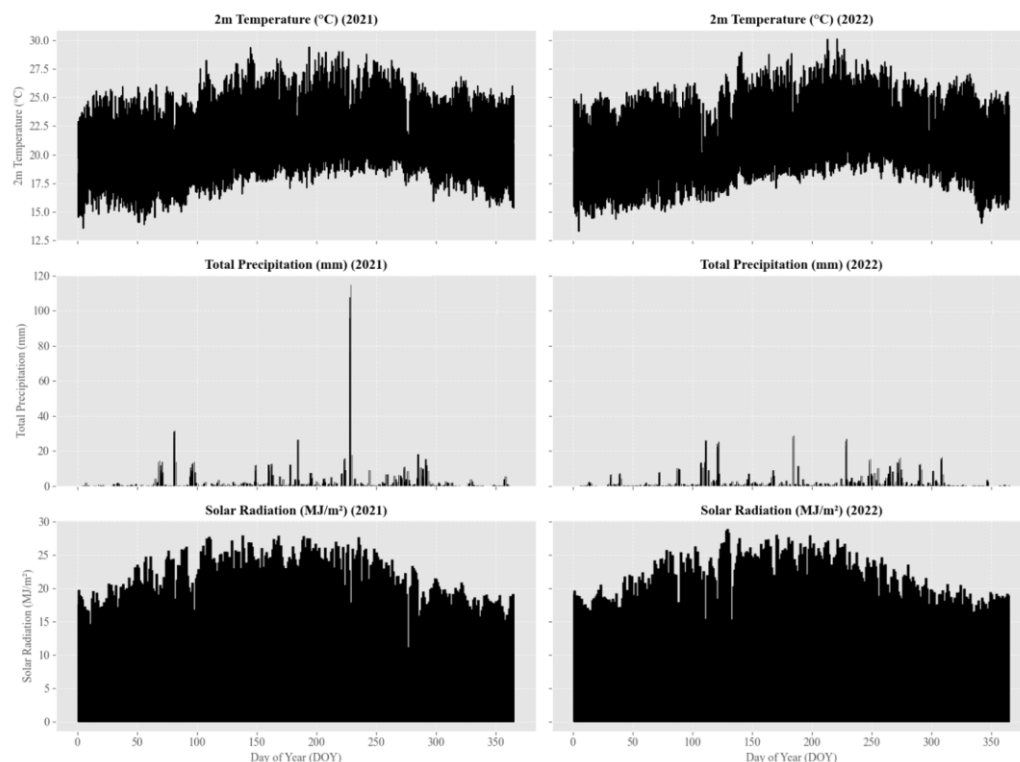

Figure 4. Daily variations in temperature, precipitation, and solar radiation for 2021 and 2022.

Seasonal Variability of Meteorological Variables

Boxplots were employed to summarize the seasonal distributions of temperature, total precipitation, and solar radiation, offering a clear overview of the variability in these meteorological variables across both years (Figure 5). For the temperature, the interquartile range remained similar in both 2021 and 2022, with median temperatures slightly above 20 °C; however, the data showed considerable fluctuations, reflecting daily temperature changes. Precipitation exhibited high skewness, with most daily measurements showing minimal or no rainfall, while extreme outliers represented significant rainfall events that occurred sporadically throughout the year. This variability underscores the challenges of managing irrigation during dry weather interrupted by heavy rainfall. Solar radiation followed a similar seasonal pattern in both years, with higher values in the dry season and lower values in the wet season. The interquartile range and median values were comparable across both years, demonstrating the consistency of solar radiation throughout the growing seasons.
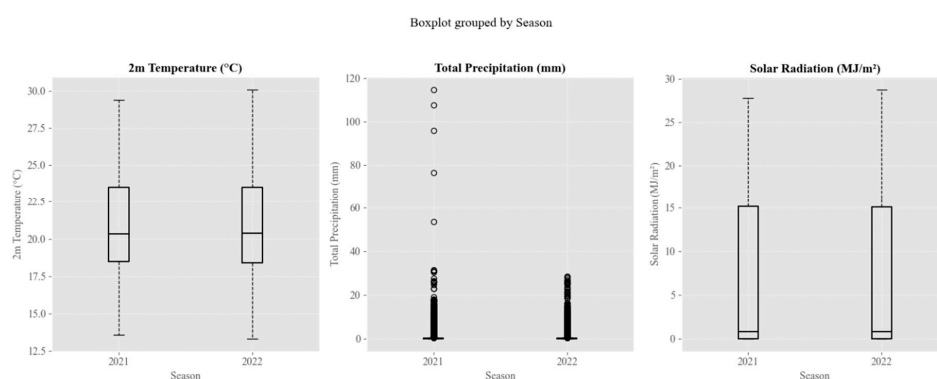
Figure 5. Temperature, precipitation, and solar radiation variability for 2021 and 2022.

3.2. Validation of Satellite-Derived Soil Moisture

Validating the satellite-derived soil moisture was critical in assessing the reliability of remote sensing technologies for monitoring soil water dynamics in the avocado orchard. This analysis compared field-measured soil moisture data with satellite estimates to evaluate the effectiveness of satellite-based soil moisture assessments, particularly for different soil depths (30 cm, 60 cm, and 120 cm). The statistical significance of the Pearson correlation coefficients (r) was consistently evaluated throughout the analyses, using a threshold of $p < 0.01$. Correlations meeting this threshold are identified with an asterisk (*) in Table 1.

Table 1. Top 10 and bottom 10 correlations between field-measured soil moisture data and satellite-derived estimates for 2021 and 2022 seasons.

Top 10 Sensor Correlations			Bottom 10 Sensor Correlations		
Rank	**Sensor**	**Correlation (r)**	**Rank**	**Sensor**	**Correlation (r)**
1	L-S5-30	0.8237 *	41	G-S7-12	−0.147
2	I-S6-60	0.7867 *	42	C-S6-60	−0.1464
3	F-S8-30	0.7297 *	43	H-S4-12	−0.1358
4	I-S8-30	0.7189 *	44	H-S2-30	−0.1341
5	M-S5-30	0.6949 *	45	F-S5-30	−0.1329
6	H-S7-12	0.6828 *	46	H-S3-60	−0.1189
7	J-S6-60	0.6615 *	47	J-S3-60	−0.106
8	H-S5-30	0.659 *	48	B-S2-30	−0.1054
9	L-S7-12	0.6448 *	49	O-S6-60	−0.1039
10	E-S8-30	0.6319 *	50	B-S3-60	−0.1022

* Statistically significant at $p < 0.01$.

Field vs. Satellite Soil Moisture

A detailed comparison was conducted between field-measured soil moisture data obtained from sensors at three different soil depths (30 cm, 60 cm, and 120 cm) and satellite-derived estimates. The comparison revealed that the strongest correlations between field and satellite data occurred at a depth of 30 cm for both the 2021 and 2022 seasons (Table 1).

The correlation analysis supports the hypothesis that the 30 cm depth is particularly effective for capturing soil moisture dynamics, as it reflects both near-surface soil moisture variations and deeper water retention, which can be effectively monitored through remote sensing.

The variability in correlations between soil moisture sensor data and satellite-derived estimates across depths likely reflects differences in sensor placement and environmental factors. Shallow sensors show stronger correlations with remote sensing data due to their sensitivity to surface-level moisture changes influenced by precipitation and evapotranspiration. In contrast, deeper sensors reflect longer-term hydrological trends less influenced by short-term meteorological conditions. Differences in soil texture and microclimate further contribute to water retention and drainage variability across soil depths. While these aspects were not the primary focus of this study, they underscore the complexity of integrating field and satellite data.

In contrast, sensors with weaker or negative correlations, such as G-S7-12 and B-S3-60, showed lower accuracy in capturing soil moisture variations, emphasizing the importance of selecting the appropriate sensor depth and configuration for reliable data acquisition.

The previous analysis is complemented by Figure 6, which visually highlights the performance of the top 10 and bottom 10 sensors based on their correlations with satellite-derived soil moisture data from the 2021 and 2022 seasons. The bar plots on the left depict the sensors with the highest positive correlation coefficients, emphasizing those that closely align with satellite measurements, while the plots on the right display the sensors with the lowest or negative correlation coefficients, indicating a weaker or inverse relationship.

For 2021, the sensor L-S5-30 at a depth of 30 cm stands out as the best-performing sensor, with a correlation coefficient of 0.8237, further reinforcing the finding that sensors positioned at this depth are optimal for capturing reliable soil moisture data that are comparable to satellite observations. Other sensors at 30 cm, such as F-S8-30 and I-S8-30, also demonstrate strong correlations, confirming the significance of this depth. For the 2022 season, the A-S7-12 sensor exhibits the highest correlation coefficient, albeit lower than the top values observed in 2021. Despite this, sensors at 30 cm, such as A-S2-30 and A-S1-30, continue to perform among the best, supporting the hypothesis that this depth is consistently adequate across different seasons.
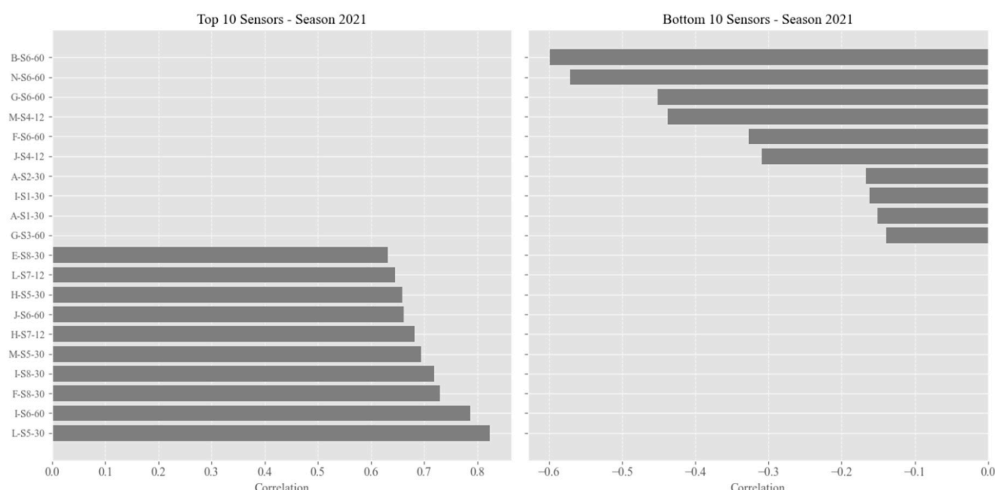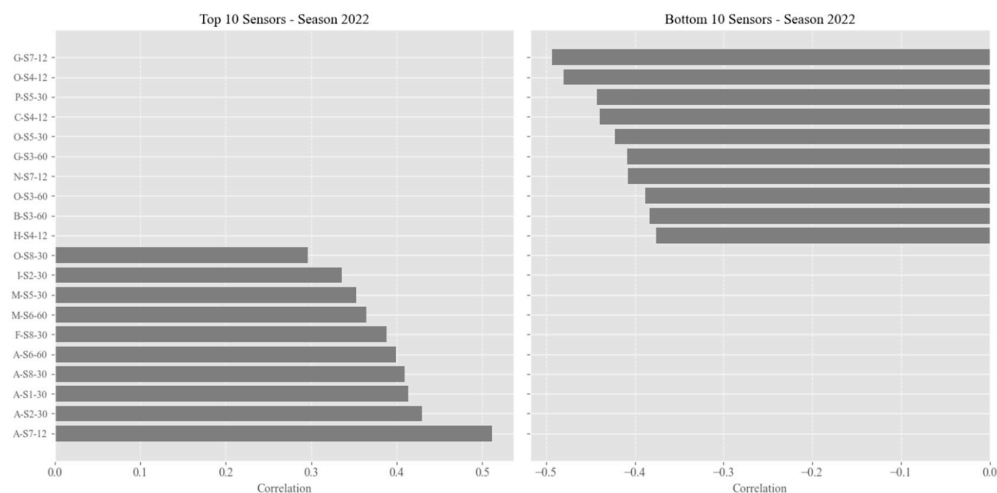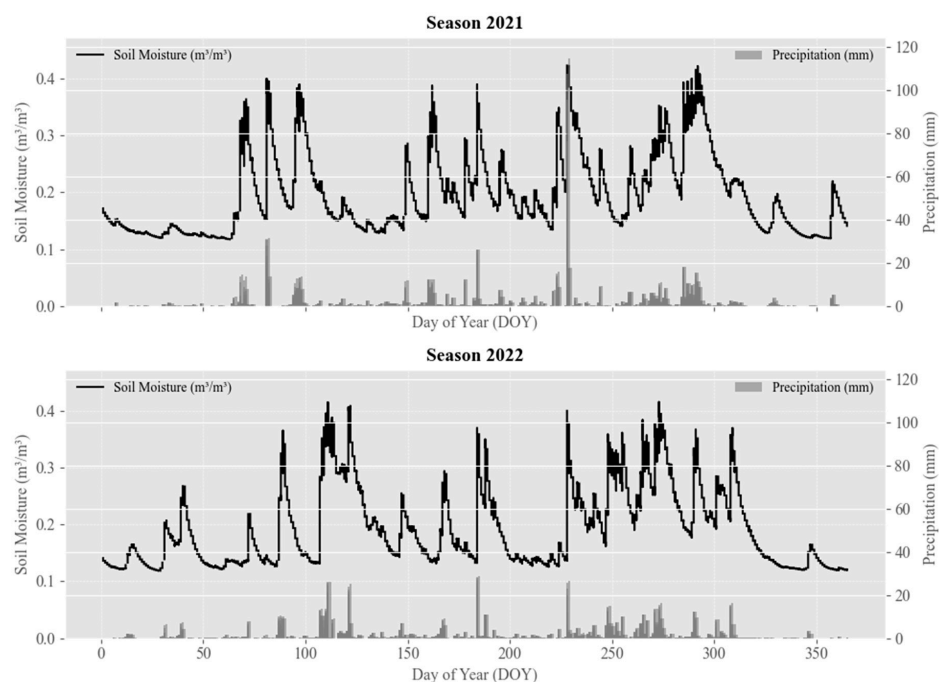

Figure 6. *Cont.*

Figure 6. Top- and bottom-performing sensors: correlation analysis with satellite data (2021–2022).

The bottom 10 sensors for both seasons show significantly lower or negative correlation coefficients, indicating discrepancies between field measurements and satellite estimates. These results highlight the variability in sensor performance based on placement and environmental conditions. This visualization provides a comprehensive overview of the most and least effective sensors, aligning with the conclusion that a 30 cm depth consistently yields the most reliable data for satellite validation.

Temporal Dynamics

Satellite-derived soil moisture data were compared with precipitation records to analyze the temporal dynamics of soil moisture fluctuations. Figure 7 illustrates this comparison, with soil moisture data (black line) overlaid on precipitation data (gray bars). The analysis revealed that satellite data effectively captured soil moisture fluctuations following precipitation events, with notable increases in soil moisture levels immediately after rainfall.


Figure 7. Satellite-based soil moisture and precipitation by season (2021–2022).

For the 2021 season, the soil moisture data show a strong response to precipitation events, with notable increases following rainfall. Periods of high precipitation correspond to sharp rises in soil moisture, which gradually declines during dry periods, reflecting typical hydrological processes. Similarly, the 2022 season exhibits consistent patterns, with soil moisture levels closely tracking precipitation events. However, variations in the magnitude of soil moisture compared to 2021 may indicate differences in the seasonal rainfall intensity, distribution, or land surface conditions. These results suggest that integrating meteorological precipitation records further enhances the understanding of soil moisture fluctuations, emphasizing the satellite data's applicability for large-scale and long-term environmental monitoring. In addition to this, it also highlights the reliability of remote sensing technologies for capturing soil moisture dynamics on a broader temporal scale.

3.3. Seasonal Trends in Vegetation Indices

The analysis of vegetation indices—the NDVI, NDWI, and SAVI—offers valuable insights into the seasonal dynamics of vegetation health, water contents, and overall productivity in the avocado orchard. These indices are essential tools for understanding the temporal fluctuations in vegetative cover, crucial for assessing plant water stress and optimizing irrigation strategies in remote agricultural areas.

Figure 8 shows the seasonal trends of the NDVI, NDWI, and SAVI over the 2021 and 2022 growing seasons. Each index is presented with its mean value (solid line) and variability (shaded standard deviation) throughout the days of the year (DOY). This temporal analysis allows for a characterization of the seasonal changes in vegetation health and water contents, offering a comprehensive understanding of the vegetative dynamics across both years.
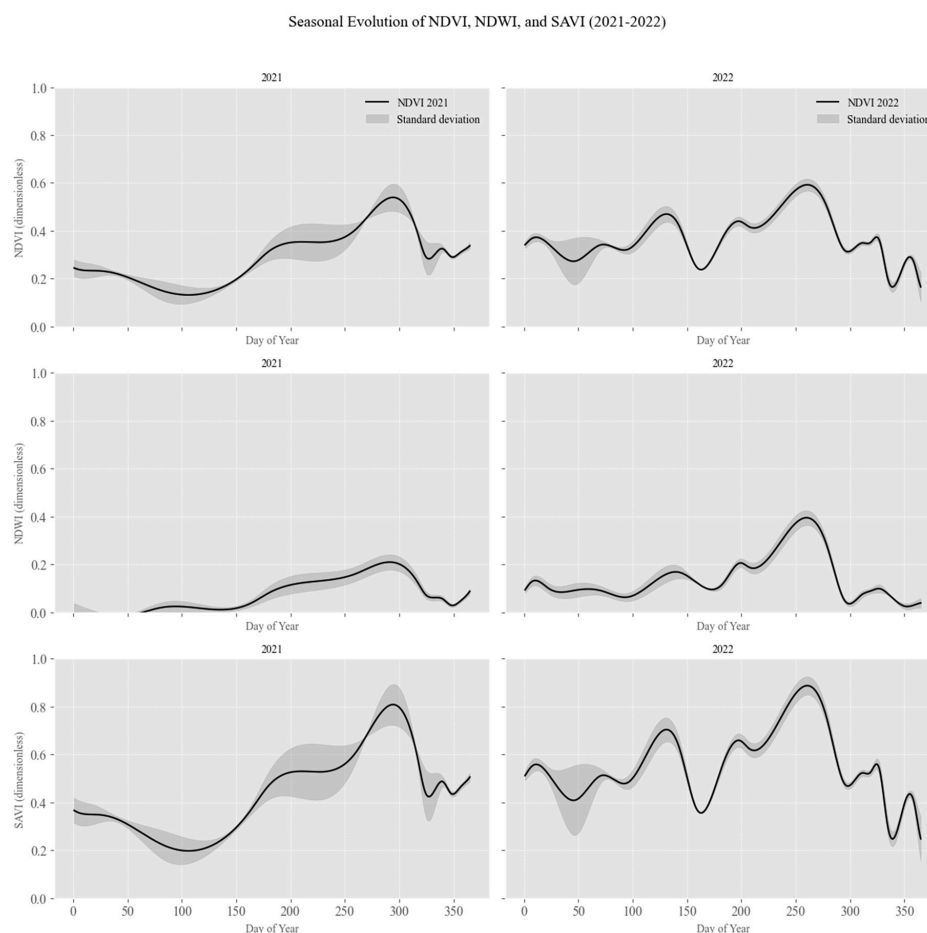
Figure 8. Seasonal evolution of vegetative expression using NDVI, NDWI, and SAVI (2021–2022).

The NDVI is widely used to assess canopy greenness and vegetative vigor, and it follows a clear seasonal pattern. It gradually increased during the early months of 2021 and 2022, reflecting the active growth phase of the avocado trees. The peak NDVI values observed in the middle of the growing season indicate maximum canopy greenness and optimal vegetative health, while a subsequent decline towards the end of the season aligns with the senescence phase or harvest periods. This trend demonstrates that the NDVI is highly responsive to vegetation growth and environmental conditions, making it a reliable tool for monitoring crop health over time. Similarly, the NDWI measures dynamic changes in the canopy water content, showing low values early in the season as the vegetation is in its early growth stages. As the season progresses, the NDWI values rise, particularly during the wettest periods when the vegetation reaches its peak water content. The highest NDWI values correspond to the wet season, while a decline during the dry season reflects reduced water availability or vegetation decline. These fluctuations emphasize the NDWI's sensitivity to vegetative growth and water availability, making it an effective indicator of plant water stress. The SAVI, which accounts for the soil's influence in areas with sparse vegetation, follows a similar pattern to the NDVI but provides more comprehensive insights into variations in vegetative cover, especially during transitions between growth and senescence. The peak in SAVI values during the middle of the growing season indicates robust vegetation and healthy canopy cover. At the same time, the index also captures finer variations in vegetative density, offering valuable information for assessing canopy health in agricultural systems with varying levels of vegetation.

These indices collectively reflect the phenological patterns of vegetation, emphasizing the key periods of vegetative growth, maximum productivity, and decline. Their consistent seasonal trends across both years demonstrate their reliability as tools for monitoring vegetative expression and ecosystem dynamics in the avocado orchard. Integrating the NDVI, NDWI, and SAVI in this analysis offers a comprehensive view of vegetation health and water contents. This is critical for water management and irrigation optimization, particularly in remote agricultural areas with limited access to ground-based monitoring.

While the seasonal variation trends observed in vegetation indices such as the NDVI, NDWI, and SAVI effectively capture general crop responses to water availability, this study acknowledges the practical implications of the observed fluctuation ranges between the dry and wet seasons. Specifically, these fluctuations may significantly impact orchard crops, influencing their phenological development, yield potential, and susceptibility to stress. Although a direct comparative analysis with other similar study areas or crops was not conducted, the methodology and results align with established findings in tropical agricultural systems.

3.4. Crop Coefficients (Kc) Derived from NDVI, NDWI, and SAVI

The calculation of Kc based on the NDVI provided valuable insights into the seasonal and spatial variability of water requirements for the avocado orchard. The relationship between Kc and the NDVI was used to derive seasonal trends in crop water dynamics, directly linking changes in vegetation health and canopy development to the crop's water needs.

Figure 9 illustrates the seasonal evolution of Kc, derived from the NDVI, for both the 2021 and 2022 growing seasons. The graphs depict the Kc values calculated from the NDVI, NDWI, and SAVI across both years, providing a comprehensive understanding of crop water dynamics. Each index reveals distinct patterns of temporal variability corresponding to changes in vegetative growth, water availability, and phenological stages.
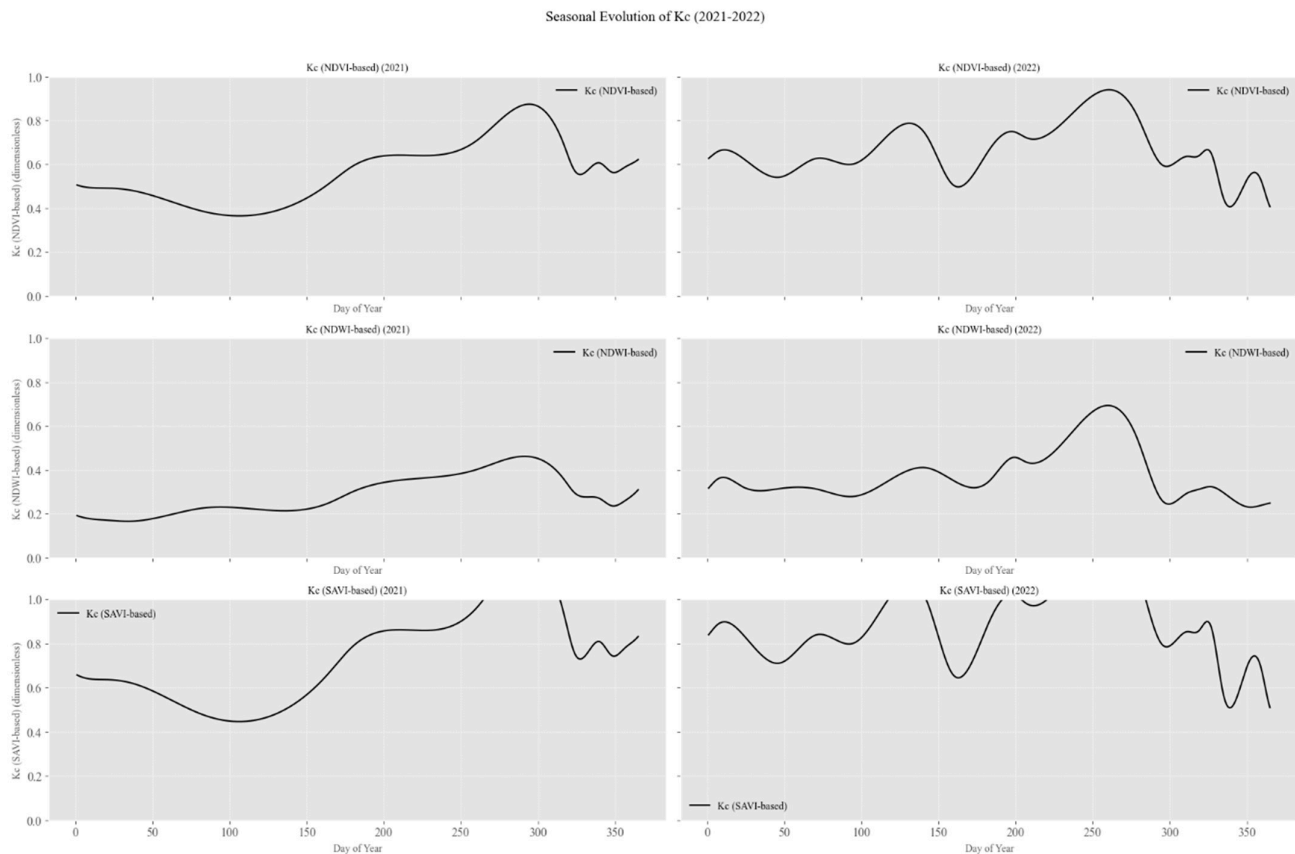
Figure 9. Kc values calculated using the Kc-NDVI relation for the three indices.

The Kc-NDVI relationship shows a clear seasonal trend, with Kc values increasing during the early stages of crop growth as the canopy develops and the vegetation becomes more vigorous. This increase is followed by a peak during the mid-growing season, aligning with the period of maximum canopy cover and vegetative health. Subsequently, Kc values decline towards the end of the growing season as the crop experiences senescence or harvest periods. This pattern is consistent across both 2021 and 2022, with some variations in the magnitude of Kc due to seasonal differences in rainfall, temperature, and other climatic factors.

The Kc values derived from the NDVI reflect the dynamic relationship between vegetation growth and water availability. Higher Kc values during active growth indicate increased water demand, while lower values correspond to reduced crop water requirements during the later stages of the growing season. These findings underscore the importance of NDVI-based crop coefficients in assessing water stress and optimizing irrigation schedules in avocado orchards, particularly in regions with limited access to ground-based monitoring data.

The spatial variability of Kc values across different areas of the orchard further highlights the heterogeneity of water requirements within the study area. This variability was influenced by the soil texture, vegetation density, and local microclimatic conditions, which affect how water is distributed and retained within the orchard. Integrating Kc values with satellite-derived soil moisture and precipitation data provides a more robust and comprehensive understanding of the orchard's water dynamics, facilitating better water management practices in regions with limited technological infrastructure.

3.5. Reference Evapotranspiration (ETo) Estimates

Estimating ETo is essential for understanding the water requirements of the avocado orchard, particularly for developing irrigation strategies that are responsive to seasonal

changes in climate. ETo estimates were derived using three meteorological models: the Hargreaves–Samani, Blaney–Criddle, and Priestley–Taylor models. These models provided a range of estimates, each with strengths and limitations, making it crucial to analyze their seasonal trends and the variability in ETo values across the different methods.

The seasonal trends in ETo calculated using the three different models for the 2021 and 2022 growing seasons are shown in Figure 10. The upper panels show the seasonal variation in ETo estimates derived from the Hargreaves–Samani model, which shows considerable fluctuations across both years. The middle panels display the forecast from the Blaney–Criddle model, which presents a more consistent seasonal trend with lower variability. The lower panels depict the estimates from the Priestley–Taylor model, which, similarly to the Blaney–Criddle model, shows a smooth seasonal curve with minimal fluctuation.
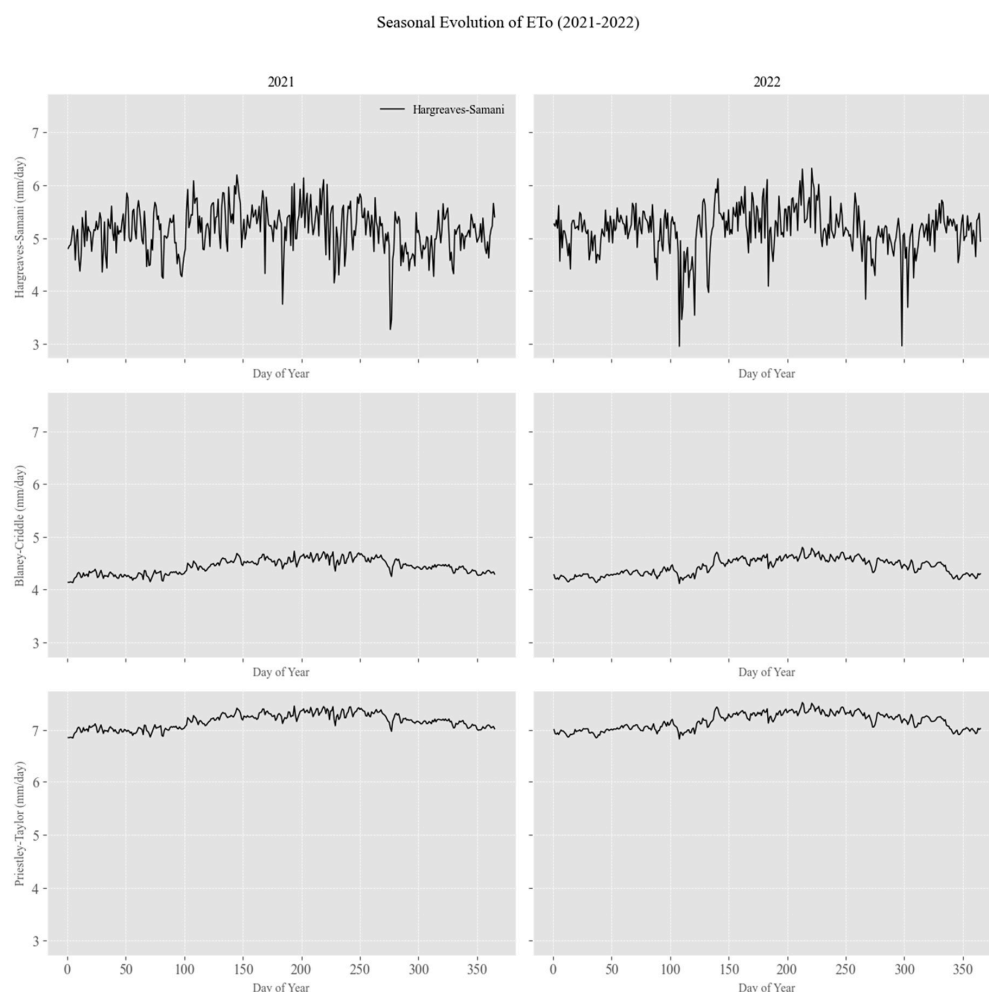
Figure 10. Seasonal evolution of ETo using three models (2021–2022).

- Hargreaves–Samani Model: This model, which relies primarily on temperature data, showed higher variability in its ETo estimates than the other models. The fluctuations in the estimates were more pronounced, especially in response to temperature changes. While this model is often used in data-scarce regions, its performance under tropical conditions showed limitations, particularly in capturing the nuances of water demand during the wetter and drier phases of the growing season. Despite this, the Hargreaves–Samani model remains helpful in regions with scarce high-quality wind speed and humidity data.
- Blaney–Criddle Model: The Blaney–Criddle model provided a more consistent estimate of ETo, with lower variability than the Hargreaves–Samani model. This model,

relying on temperature and daylight data, showed a smooth seasonal curve, offering stability in estimating ETo across both years. However, it may not capture rapid changes in water demand driven by short-term fluctuations in temperature or other environmental factors.

- Priestley–Taylor Model: Like the Blaney–Criddle model, the Priestley–Taylor model demonstrated stable estimates with lesser fluctuation. It is particularly effective in humid regions, where its assumptions about the proportionality between energy availability and evapotranspiration hold more accurately. However, it showed some limitations during the dry periods of the seasons when its estimates did not reflect the sharp fluctuations observed in the field data.

4. Discussion

4.1. Validity of Satellite-Derived Soil Moisture

The comparison of field-measured soil moisture data and satellite-derived estimates confirmed the effectiveness of remote sensing technologies in monitoring soil water dynamics in avocado orchards. The strongest correlations between field measurements and satellite data were consistently observed at the 30 cm depth, corresponding to the root zone dynamics of avocado trees. This depth is critical as it represents the upper portion of the root zone, where most water uptake occurs, especially during irrigation and evaporation processes.

Performance of 30 cm Depth Sensors

The 30 cm depth demonstrated the strongest correlation with satellite-derived soil moisture data, with a correlation coefficient of 0.8237 in 2021. This depth reflects the most dynamic zone of soil moisture variation due to its proximity to the root zone, which is most sensitive to changes in irrigation and rainfall [43]. Root uptake is most active in this zone, playing a significant role in determining the immediate water availability for plants [44]. This dynamic behavior of the 30 cm depth likely explains its strong correlation with the satellite data, as it captures the surface-level water availability most influenced by seasonal changes, irrigation practices, and evaporation processes.

The high performance at this depth is also consistent with the findings in other agricultural studies that indicated that shallow soil layers are more responsive to short-term changes in environmental conditions [28], such as precipitation and irrigation, which remote sensing technologies can detect. For instance, similar results were observed in studies of vineyards and other high-water-demand crops, where satellite-derived soil moisture values showed strong correlations with field measurements at depths ranging from 30 cm to 60 cm [45,46]. These studies support the relevance of a 30 cm depth for effective satellite-based soil moisture monitoring, especially in the context of surface-level water availability.

Temporal and Spatial Accuracy

The ERA5-derived soil moisture estimates effectively captured soil moisture dynamics during the wet and dry seasons, as also shown in other studies [47,48]. These satellite-derived soil moisture estimates closely tracked fluctuations in field-based measurements, especially following precipitation events. This temporal alignment demonstrates that ERA5 data are sensitive to seasonal transitions, providing valuable insights into the water availability and irrigation needs of avocado orchards [49,50].

However, while ERA5 data effectively capture general trends in soil moisture, their spatial resolution limits their ability to capture fine-scale variability within an orchard, particularly in areas with heterogeneous soil textures or microclimates [51]. Previous studies have also pointed out that higher-resolution satellite data or additional ground-based measurements might be needed to refine soil moisture estimates at the field level.

For instance, in a prior study [52], the authors emphasized that traditional satellite data often lack the spatial detail necessary for accurate soil moisture estimation, particularly at the field level, and highlighted the importance of integrating ground-based measurements to improve accuracy and representativeness in agricultural contexts. Another study [53] noted that the original spatial resolution of satellite platforms is insufficient for agricultural applications, which require higher spatial detail, suggesting the combination of satellite data with ground-based measurements to achieve more precise soil moisture estimates. In this sense, the spatial variability observed in this study could not be fully captured by the ERA5 data, suggesting that more precise monitoring might require denser sensor networks or higher-spatial-resolution satellite imagery. Overall, integrating ERA5 soil moisture data with ground-based field measurements provided a robust framework for assessing soil water dynamics in the avocado orchard. While the ERA5 data captured broader trends in soil moisture, improvements in spatial resolution and sensor deployment strategies could enhance the detection of fine-scale variability.

Vegetation Index Performance Across Seasons

The NDVI, SAVI, and NDWI analysis revealed significant insights into the seasonal dynamics of vegetation health, growth stages, and water availability in the avocado orchard. The NDVI and SAVI were particularly useful for tracking the vegetative growth phases and canopy greenness [54,55]. At the same time, the NDWI proved to be an effective tool for monitoring the water content in the vegetation, thereby providing insights into plant water stress.

Both the NDVI and SAVI showed clear seasonal patterns, where the NDVI exhibited a gradual increase during the early months of the 2021 and 2022 growing seasons, reflecting the active vegetative growth of the avocado trees. The peak in NDVI values, occurring in the middle of each growing season, signaled maximum canopy greenness, corresponding to periods of high photosynthetic activity and optimal vegetative health [56,57]. This increase in the NDVI was followed by a decline towards the end of the season, likely due to senescence or the harvest period [58], a common phenological change in fruit-bearing crops like avocados. The SAVI, which accounts for the soil's influence in sparsely vegetated areas, showed a similar seasonal trend, reinforcing its utility in monitoring vegetation cover in orchards with partial canopy coverage.

In contrast, the NDWI was more sensitive to changes in water contents within the vegetation canopy. The NDWI values were generally low during the early stages of the growing season, corresponding to periods of minimal water availability. As the season progressed, the NDWI values increased, peaking during the wettest months when the vegetation was at its maximum water content. These increases in the NDWI were particularly evident during the wet season, highlighting the sensitivity of this index to fluctuations in water availability. The reduction in the NDWI during dry periods served as a clear indicator of water stress, making this index a valuable tool for monitoring the water status of crops.

This analysis provided valuable insights into how vegetation responds to changing weather conditions, such as periods of water stress or growth phases. It contributed to understanding the interactions between vegetation health and soil moisture dynamics. Integrating these satellite-derived vegetation indices allowed for a comprehensive assessment of the orchard's seasonal dynamics.

Phenological Patterns, Environmental Drivers, and Integration with Field Data

The seasonal trends in vegetation indices (NDVI, SAVI, and NDWI) reflected the phenological stages of the avocado crop and its response to environmental factors such as temperature and precipitation. During the growing season, peak NDVI values coincided

with the period of maximum vegetative growth, which aligned with favorable temperature and soil moisture conditions [59], as expected in temperate climates. Meteorological variables, particularly high temperatures and low precipitation during the dry season, significantly influenced the vegetation index dynamics [60]. These conditions contributed to a decline in vegetation indices towards the end of the year, indicating stress experienced by the trees. The temperature and VPD increase during dry periods heightened the atmospheric water demand, leading to higher evapotranspiration rates and reduced soil moisture availability. This was evident in the decline in the NDWI, which signaled water stress, particularly during dry spells, where high VPD values further intensified the effect.

The relationship between precipitation and the NDWI was particularly noteworthy, as increases in moisture content following rainfall events correlated with sharp rises in NDWI values [61,62]. This demonstrates the NDWI's effectiveness as a reliable indicator of water availability and plant water stress. The interplay between meteorological factors and vegetation indices illustrates the complex dynamics of crop growth and water availability, which can be captured using remote sensing tools [63]. However, discrepancies were noted between satellite-derived vegetation indices and field-measured soil moisture, particularly during transitions between wet and dry periods. Field measurements provided more granular insights into the spatial variability of soil moisture across the orchard, which the satellite data could not fully capture due to their 30 m resolution. Microclimatic factors such as soil texture, slope, and shading likely contributed to this variability, resulting in discrepancies between field data and satellite estimates. For example, areas with dense canopy coverage showed higher NDVI and SAVI values but experienced localized water stress due to limited irrigation or soil moisture retention variations. These observations highlight the importance of integrating satellite data with field measurements for a more accurate and reliable assessment of crop water status, particularly in areas with spatial variability that remote sensing alone cannot capture.

4.2. Crop Coefficients (Kc) Derived from NDVI: Relevance of Kc Variability

The seasonal variability of Kc derived from the NDVI provided a more accurate representation of the water requirements for the avocado orchard. The Kc values, derived from the NDVI, followed clear seasonal trends that mirrored the vegetative phases of the avocado trees. Peak Kc values coincided with the maximum canopy greenness observed in the middle of the growing season, indicating a period of high water demand. This is consistent with the findings from the literature that crop water requirements are highest during peak vegetative growth, which aligns with the observed increase in Kc. For instance, in a prior study [64], the authors aimed to enhance evapotranspiration estimates by integrating NDVI-derived Kc for precise water management in croplands; they noted that NDVI-derived Kc was able to effectively reflect the crop water demand, aligning with water stress indicators by capturing vegetation health and growth dynamics and becoming an aid in precision irrigation and stress mitigation. The advantage of using the satellite-derived NDVI to calculate Kc is the ability to derive dynamic, spatially explicit Kc values responsive to seasonal changes in vegetation health and water availability [65,66]. These values offer a more detailed and accurate estimate of water requirements than the static tabular values typically used in traditional irrigation scheduling. In contrast to standard Kc values, which are fixed for specific crop types and growth stages, the NDVI-based Kc values reflect the actual condition of the vegetation, adjusting in real time to changes in canopy development, soil moisture, and weather conditions.

Moreover, the Kc values derived from the NDVI, SAVI, and NDWI were validated by comparing them with published values for avocado orchards in similar agroecological conditions. The estimated Kc values were also analyzed alongside soil moisture data

to ensure consistency with field observations. The agreement between the vegetation-index-derived Kc values and seasonal water stress patterns observed in soil moisture measurements supports the applicability of these empirical relationships for irrigation management.

Despite these advantages, the use of VIs and WIs for estimating Kc presents certain limitations that must be considered, given that the accuracy of Kc estimations derived from remote sensing data can be influenced by several environmental and agronomic factors such as the following: (i) Variety differences: Different avocado cultivars exhibit variations in their canopy structure, leaf area index (LAI), and stomatal conductance, which may affect the spectral response captured by the NDVI, SAVI, and NDWI. As a result, the empirical equations used to derive Kc from these indices may require calibration to account for varietal differences. (ii) Soil type influence: Soil texture and composition impact water retention, infiltration rates, and root-zone moisture availability, affecting how vegetation indices reflect the actual water status. For instance, in areas with heterogeneous soil properties, additional calibration or integration with soil moisture measurements may be required. (iii) Climate variability: Meteorological conditions such as the temperature, humidity, and wind speed influence the water-use efficiency and evapotranspiration rates; therefore, the spectral response of VIs and WIs may vary under extreme climatic conditions (e.g., prolonged droughts or excessive rainfall), potentially affecting Kc estimations.

Implications for Irrigation Scheduling

Seasonally varying Kc values derived from the NDVI can significantly enhance irrigation efficiency, especially under water-limited conditions. Using dynamic Kc values, irrigation schedules can be more accurately tailored to the crop's actual water needs, reducing water waste during less demanding periods and ensuring adequate irrigation during high-demand phases, such as the mid-growing season. This dynamic approach to irrigation management is especially beneficial in regions facing water scarcity, where efficient water use is critical for sustaining crop health and productivity. The Kc values derived from the NDVI in this study demonstrated their usefulness in capturing the water demand of the avocado crop, providing an adaptive tool for precision irrigation. These values were closely aligned with the phenological stages of the crop, highlighting the relationship between vegetation growth and water needs. The ability to adjust irrigation schedules based on real-time Kc estimates derived from remote sensing data represents a substantial advancement in precision agriculture, particularly for crops like avocados, which are highly sensitive to water stress.

4.3. Reference Evapotranspiration (ETo) Estimates

The comparison of three ETo models—Hargreaves–Samani, Blaney–Criddle, and Priestley–Taylor—revealed notable differences in their performance in estimating the water demand of the avocado orchard. Each model employs distinct approaches and parameterizations, influencing their applicability and accuracy under varying environmental conditions. Our analysis indicated that while all three models can estimate ETo, their performance varies depending on the local climatic factors and the available meteorological data.

The Hargreaves–Samani model, based primarily on temperature data, showed higher variability in its ETo estimates, particularly during rapid temperature changes. While commonly used in areas with limited meteorological data, its performance in tropical conditions revealed limitations, particularly in capturing the nuances of water demand during the wet and dry phases of the growing season. Similar observations were made by the authors of [67], who indicated that while the Hargreaves–Samani model is accurate and uses readily available data, its accuracy is low when geographical and climatic conditions vary. However, this model remains helpful in regions where high-quality wind speed and

humidity data are unavailable. This is similar to what was observed by the authors of [68], who indicated that this model is very precise for the estimation of ETo, especially if it is used in combination with agrometeorological information from ERA5-land, which is an enhanced version of ERA5.

The Blaney–Criddle model, which relies on temperature and daylight hours, provided a more consistent estimate of ETo throughout the growing season. This model is more straightforward and effective in regions where solar radiation data may not be available, making it a practical choice for areas with limited meteorological infrastructure. However, its estimates could have been more precise during extreme conditions, such as rapid changes in temperature or varying precipitation, highlighting its limitations under tropical conditions.

The Priestley–Taylor model, like the Blaney–Criddle model, showed lower variability in its estimates compared to the Hargreaves–Samani model. This aligns with findings by the authors of [69], who noted that the coefficients of this model displayed little variation across four regions, suggesting its potential for ETo calculation. It uses solar radiation as the primary factor for evapotranspiration, making it well suited for humid regions where energy-driven evapotranspiration dominates. However, its accuracy during drier months could have been more reliable, as it needed to fully account for changes in water availability driven by temperature fluctuations and relative humidity. This limitation underscores the importance of selecting the most appropriate model based on the local climate and available meteorological parameters.

In practice, accurate ETo estimates, particularly from the Blaney–Criddle and Priestley–Taylor models, combined with the Kc values derived from the NDVI, provided a robust framework for estimating the crop water demand in the avocado orchard. This study was able to estimate crop water needs more precisely across different phenological stages by integrating satellite-derived vegetation indices with reference evapotranspiration values. This combination offers a more data-driven approach to irrigation, allowing for real-time adjustments based on the crop's actual water needs and environmental conditions.

Each ETo model in this study presents strengths and limitations depending on the climatic conditions. The Hargreaves–Samani model, while suitable for data-limited regions, may underperform in humid conditions where additional climatic factors like humidity and wind speed play a role. The Blaney–Criddle model provides a stable estimate but may lack responsiveness to sudden changes in precipitation and temperature. The Priestley–Taylor model performs well in humid environments but may not fully account for advection effects in dry conditions. Understanding these limitations is crucial for selecting appropriate ETo models in different climatic contexts and ensuring the robustness of irrigation recommendations.

Selecting the appropriate ETo model depends on specific climatic conditions and the availability of meteorological data. For arid and semi-arid regions, the Hargreaves–Samani model is preferred due to its reliance primarily on temperature data, which are commonly available in such environments. In contrast, for humid climates, the Priestley–Taylor model is more suitable as it accounts for the energy balance, which plays a significant role in these areas. The Blaney–Criddle model is recommended for temperate climates, where additional meteorological data, such as wind speed and humidity, are available, allowing for more accurate estimates. We also acknowledge the limitations of these models, particularly in terms of their spatial and temporal resolution, which may impact their applicability in regions with complex microclimates. To address these limitations, we suggest incorporating high-resolution satellite data to refine the accuracy of the models. Additionally, we highlight the importance of local calibration and validation of these models to ensure their accuracy in specific agroecological conditions. Lastly, we propose that future research focus on

integrating machine learning techniques with traditional ETo models, which could improve their adaptability and predictive capabilities across different agricultural regions.

Integrating ETo models with NDVI-derived Kc values enabled the dynamic management of crop water requirements. By adjusting irrigation schedules based on seasonally varying Kc values, this study demonstrated how irrigation practices could be refined to ensure that water is applied efficiently, reducing the risk of over- or under-irrigation. However, the variability in ETo estimates among the models highlights the importance of selecting the right model for specific irrigation decisions. The differences observed among the Hargreaves–Samani, Blaney–Criddle, and Priestley–Taylor models, especially during the dry season, suggest that relying solely on one model in regions with significant seasonal changes in temperature and precipitation could lead to less efficient water use.

4.4. Implications for Agricultural Water Management

Scalability of Satellite-Based Approaches

The findings from this study suggest that satellite-based approaches for monitoring crop water stress and optimizing irrigation management can be effectively applied to other tropical crops or regions facing similar water management challenges. Integrating satellite-derived vegetation indices, such as the NDVI, NDWI, and SAVI, with ground-based soil moisture sensors has proven to be a reliable method for assessing water stress in avocado orchards, and this methodology holds excellent potential for broader application. Tropical crops such as bananas, citrus, and mangoes, which similarly experience high water demands and are sensitive to water stress, can benefit from these techniques. By adapting this approach to different crops, agriculturalists can improve water-use efficiency and crop productivity in water-scarce regions, contributing to sustainable agriculture.

Although this study was conducted on avocado orchards, the presented methodology provides valuable insights for other crops in water-scarce areas, particularly in tropical regions. We recognize that different crops have unique growth cycles and water requirements, which may influence their response to water stress. However, the relationship between vegetation indices (such as the NDVI) and water indices (such as the CWSI) remains consistent across many crops, including other tropical species, based on general physiological principles governing plant water stress. For instance, many tropical crops share similar responses to water deficits, which makes the model adaptable to other crops with some calibration. To enhance the applicability of this study to other crops, future research should focus on calibrating the model for various tropical species, taking into account their specific growth cycles and water needs. This would involve validating the model against various crops under varying climatic conditions, allowing for fine-tuning of the parameters to ensure that crop-specific characteristics do not negatively impact the model's effectiveness. Additionally, we propose further field trials to test the model's scalability to a broader range of tropical crops, ensuring its robustness and adaptability.

Although this study primarily relied on vegetation indices and soil moisture sensors to assess water stress, we recognize that additional factors such as soil texture, topography, and microclimate variations influence crop water availability. Future studies could benefit from incorporating high-resolution soil maps and localized meteorological models, enhancing the precision of water stress assessments and irrigation recommendations. Such approaches would enable more site-specific hydrological analysis, thus improving precision agriculture decision-making.

Moreover, the scalability of this approach is supported by the availability of global satellite data, such as Landsat 8 and 9 imageries, which offer free access to consistent, high-resolution data for vegetation monitoring. This cost-effectiveness makes satellite-based methods an attractive alternative to traditional, resource-intensive irrigation manage-

ment systems, especially in regions where financial and logistical constraints hinder the widespread use of ground-based sensors. With minimal field validation required, satellite-based data can provide large-scale insights into water dynamics, allowing for real-time adjustments to irrigation schedules across vast areas, potentially improving water resource management at the regional or national level.

5. Conclusions

This study comprehensively evaluated satellite-based remote sensing technologies integrated with field-based soil moisture sensors for assessing water stress in avocado orchards. The key findings highlight the effectiveness of satellite-derived vegetation indices, such as the NDVI, NDWI, and SAVI, in monitoring vegetation health. The 30 cm depth sensor data consistently correlated strongly with satellite-derived soil moisture data. Integrating these tools enabled the detection of water stress dynamics, offering an innovative and cost-effective approach to irrigation management, especially in remote agricultural areas where traditional methods are often impractical.

The results underscore the potential of using remote sensing technologies as a viable alternative to conventional irrigation monitoring systems. This study advances precision agriculture by showing how satellite-derived data and field-based soil moisture measurements can enhance water management practices, even in regions with limited access to high-resolution data and infrastructure. This approach offers a scalable solution for monitoring crop water stress across large areas, thus improving water-use efficiency and supporting sustainable agricultural practices, particularly in water-limited tropical regions. However, the study acknowledges certain limitations, such as the medium spatial resolution of satellite imagery and the limited coverage of field sensors. Future research should address these constraints by integrating higher-resolution satellite data, deploying additional field sensors, and refining the models with additional vegetation indices and climatic variables. Expanding the data's spatial and temporal coverage in future studies could enhance the accuracy of crop water stress assessments and improve irrigation scheduling. Therefore, this study highlights remote sensing technologies' promising role in avocado orchards' water stress assessment and irrigation management. It paves the way for future advancements in precision agriculture under limited-data scenarios. It provides a foundation for further research to refine and scale integrated approaches to optimize water management in worldwide agricultural systems.

Conflicts of Interest: The authors declare no conflicts of interest. The funders had no role in the study's design; in the collection, analyses, or interpretation of data; in the writing of the manuscript; or in the decision to publish the results.

References

1. Liu, X.; Liu, W.; Tang, Q.; Liu, B.; Wada, Y.; Yang, H. Global Agricultural Water Scarcity Assessment Incorporating Blue and Green Water Availability Under Future Climate Change. *Earth's Future* **2022**, *10*, e2021EF002567. [CrossRef]
2. Ingrao, C.; Strippoli, R.; Lagioia, G.; Huisingh, D. Water Scarcity in Agriculture: An Overview of Causes, Impacts and Approaches for Reducing the Risks. *Heliyon* **2023**, *9*, e18507. [CrossRef] [PubMed]
3. Rosa, L. Adapting Agriculture to Climate Change via Sustainable Irrigation: Biophysical Potentials and Feedbacks. *Environ. Res. Lett.* **2022**, *17*, 063008. [CrossRef]
4. Khondoker, M.; Mandal, S.; Gurav, R.; Hwang, S. Freshwater Shortage, Salinity Increase, and Global Food Production: A Need for Sustainable Irrigation Water Desalination—A Scoping Review. *Earth* **2023**, *4*, 223–240. [CrossRef]
5. Caffrey, P.; Kindberg, L.; Stone, C.; de Obeso, J.; Trzaska, K.; Torres, R.; Meier, G. *Dominican Republic Climate Change Vulnerability Assessment Report*; United States Agency for International Development (USAID): Washington, DC, USA, 2013.
6. Jury, M.R. Winter Climate of Northeastern Dominican Republic and Cash Crop Production. *Climate* **2023**, *11*, 161. [CrossRef]
7. Netherlands Enterprise Agency. *Ministry of Foreign Affairs Dominican Republic Agricultural Sector Report 2023*; Netherlands Enterprise Agency: The Hague, The Netherlands, 2023.
8. Cárceles Rodríguez, B.; Durán Zuazo, V.H.; Franco Tarifa, D.; Cuadros Tavira, S.; Sacristan, P.C.; García-Tejero, I.F. Irrigation Alternatives for Avocado (*Persea Americana* Mill.) in the Mediterranean Subtropical Region in the Context of Climate Change: A Review. *Agriculture* **2023**, *13*, 1049. [CrossRef]
9. Zuazo, V.H.D.; Lipan, L.; Rodríguez, B.C.; Sendra, E.; Tarifa, D.F.; Nemś, A.; Ruiz, B.G.; Carbonell-Barrachina, Á.A.; García-Tejero, I.F. Impact of Deficit Irrigation on Fruit Yield and Lipid Profile of Terraced Avocado Orchards. *Agron. Sustain. Dev.* **2021**, *41*, 69. [CrossRef]
10. Reints, J.; Dinar, A.; Crowley, D. Dealing with Water Scarcity and Salinity: Adoption of Water Efficient Technologies and Management Practices by California Avocado Growers. *Sustainability* **2020**, *12*, 3555. [CrossRef]
11. Taramuel-Taramuel, J.P.; Montoya-Restrepo, I.A.; Barrios, D. Challenges in the Avocado Production Chain in Latin America: A Descriptive Analysis. *Agron. Colomb.* **2024**, *42*, e113982. [CrossRef]
12. Beyá-Marshall, V.; Arcos, E.; Seguel, Ó.; Galleguillos, M.; Kremer, C. Optimal Irrigation Management for Avocado (Cv. 'Hass') Trees by Monitoring Soil Water Content and Plant Water Status. *Agric. Water Manag.* **2022**, *271*, 107794. [CrossRef]
13. Ahmad, U.; Alvino, A.; Marino, S. A Review of Crop Water Stress Assessment Using Remote Sensing. *Remote Sens.* **2021**, *13*, 4155. [CrossRef]
14. Virnodkar, S.S.; Pachghare, V.K.; Patil, V.C.; Jha, S.K. Remote Sensing and Machine Learning for Crop Water Stress Determination in Various Crops: A Critical Review. *Precis. Agric.* **2020**, *21*, 1121–1155. [CrossRef]
15. Gautam, D.; Pagay, V. A Review of Current and Potential Applications of Remote Sensing to Study the water Status of Horticultural Crops. *Agronomy* **2020**, *10*, 140. [CrossRef]
16. Almalki, R.; Khaki, M.; Saco, P.M.; Rodriguez, J.F. Monitoring and Mapping Vegetation Cover Changes in Arid and Semi-Arid Areas Using Remote Sensing Technology: A Review. *Remote Sens.* **2022**, *14*, 5143. [CrossRef]
17. Chen, J.; Chen, S.; Fu, R.; Li, D.; Jiang, H.; Wang, C.; Peng, Y.; Jia, K.; Hicks, B.J. Remote Sensing Big Data for Water Environment Monitoring: Current Status, Challenges, and Future Prospects. *Earth's Future* **2022**, *10*, e2021EF002289. [CrossRef]
18. Bhaga, T.D.; Dube, T.; Shekede, M.D.; Shoko, C. Impacts of Climate Variability and Drought on Surface Water Resources in Sub-Saharan Africa Using Remote Sensing: A Review. *Remote Sens.* **2020**, *12*, 4184. [CrossRef]
19. Giovos, R.; Tassopoulos, D.; Kalivas, D.; Lougkos, N.; Priovolou, A. Remote Sensing Vegetation Indices in Viticulture: A Critical Review. *Agriculture* **2021**, *11*, 457. [CrossRef]
20. Vélez, S.; Martínez-Peña, R.; Castrillo, D. Beyond Vegetation: A Review Unveiling Additional Insights into Agriculture and Forestry through the Application of Vegetation Indices. *J* **2023**, *6*, 421–436. [CrossRef]
21. Dong, H.; Dong, J.; Sun, S.; Bai, T.; Zhao, D.; Yin, Y.; Shen, X.; Wang, Y.; Zhang, Z.; Wang, Y. Crop Water Stress Detection Based on UAV Remote Sensing Systems. *Agric. Water Manag.* **2024**, *303*, 109059. [CrossRef]
22. Awais, M.; Li, W.; Cheema, M.J.M.; Zaman, Q.U.; Shaheen, A.; Aslam, B.; Zhu, W.; Ajmal, M.; Faheem, M.; Hussain, S.; et al. UAV-Based Remote Sensing in Plant Stress Imagine Using High-Resolution Thermal Sensor for Digital Agriculture Practices: A Meta-Review. *Int. J. Environ. Sci. Technol.* **2023**, *20*, 1135–1152. [CrossRef]
23. Zhou, Z.; Majeed, Y.; Diverres Naranjo, G.; Gambacorta, E.M.T. Assessment for Crop Water Stress with Infrared Thermal Imagery in Precision Agriculture: A Review and Future Prospects for Deep Learning Applications. *Comput. Electron. Agric.* **2021**, *182*, 106019. [CrossRef]

24. Eid, A.N.M.; Olatubara, C.O.; Ewemoje, T.A.; El-Hennawy, M.T.; Farouk, H. Inland Wetland Time-Series Digital Change Detection Based on SAVI and NDWI Indecies: Wadi El-Rayan Lakes, Egypt. *Remote Sens. Appl.* **2020**, *19*, 100347. [CrossRef]

25. Gueraidia, N.; Gueraidia, S.; Sirine, R.; Fehdi, C.; El Kader, H. Natural Hazard Processing Analyze Investigation Using Different Spectral (Ndvi, Ndwi, Mdwi, Savi, Ndbi, Nbr) Case Study of Souk Ahras Area-Est of Algeria. *Period. Mineral.* **2024**, *93*, 55–65.

26. Kisekka, I.; Peddinti, S.R.; Kustas, W.P.; McElrone, A.J.; Bambach-Ortiz, N.; McKee, L.; Bastiaanssen, W. Spatial–Temporal Modeling of Root Zone Soil Moisture Dynamics in a Vineyard Using Machine Learning and Remote Sensing. *Irrig. Sci.* **2022**, *40*, 761–777. [CrossRef]

27. Rasheed, M.W.; Tang, J.; Sarwar, A.; Shah, S.; Saddique, N.; Khan, M.U.; Imran Khan, M.; Nawaz, S.; Shamshiri, R.R.; Aziz, M.; et al. Soil Moisture Measuring Techniques and Factors Affecting the Moisture Dynamics: A Comprehensive Review. *Sustainability* **2022**, *14*, 11538. [CrossRef]

28. Yinglang, A.; Wang, G.; Hu, P.; Lai, X.; Xue, B.; Fang, Q. Root-Zone Soil Moisture Estimation Based on Remote Sensing Data and Deep Learning. *Environ. Res.* **2022**, *212*, 113278. [CrossRef]

29. Hu, X.; Shi, L.; Lin, G.; Lin, L. Comparison of Physical-Based, Data-Driven and Hybrid Modeling Approaches for Evapotranspiration Estimation. *J. Hydrol.* **2021**, *601*, 126592. [CrossRef]

30. Liu, Z. Estimating Land Evapotranspiration from Potential Evapotranspiration Constrained by Soil Water at Daily Scale. *Sci. Total Environ.* **2022**, *834*, 155327. [CrossRef]

31. Rouse, J.W.; Haas, R.H.; Schell, J.A.; Deering, D.W.; Harlan, J.C. *Monitoring the Vernal Advancement and Retrogradation (Greenwave Effect) of Natural Vegetation*; Texas A&M University Remote Sensing Center: College Station, TX, USA, 1974.

32. Onyia, N.N.; Balzter, H.; Berrio, J.C. Normalized Difference Vegetation Vigour Index: A New Remote Sensing Approach to Biodiversity Monitoring in Oil Polluted Regions. *Remote Sens.* **2018**, *10*, 897. [CrossRef]

33. Huete, A.R. A Soil-Adjusted Vegetation Index (SAVI). *Remote Sens. Environ.* **1988**, *25*, 295–309. [CrossRef]

34. Marino, S.; Alvino, A. Vegetation Indices Data Clustering for Dynamic Monitoring and Classification of Wheat Yield Crop Traits. *Remote Sens.* **2021**, *13*, 541. [CrossRef]

35. McFeeters, S.K. The Use of the Normalized Difference Water Index (NDWI) in the Delineation of Open Water Features. *Int. J. Remote Sens.* **1996**, *17*, 1425–1432. [CrossRef]

36. Liuzzo, L.; Puleo, V.; Nizza, S.; Freni, G. Parameterization of a Bayesian Normalized Difference Water Index for Surface Water Detection. *Geosciences* **2020**, *10*, 260. [CrossRef]

37. Zhang, L.; Zhang, H.; Niu, Y.; Han, W. Mapping Maizewater Stress Based on UAV Multispectral Remote Sensing. *Remote Sens.* **2019**, *11*, 605. [CrossRef]

38. Dhaloiya, A.; Denis, D.; Duhan, D.; Kumar, R.; Singh, M.; Malik, A. Monitoring Vegetation Health, Water Stress, and Temperature Variation through Various Indices Using Landsat 8 Data. *Indian J. Ecol.* **2023**, *50*, 802–810. [CrossRef]

39. Ashok, A.; Rani, H.P.; Jayakumar, K.V. Monitoring of Dynamic Wetland Changes Using NDVI and NDWI Based Landsat Imagery. *Remote Sens. Appl.* **2021**, *23*, 100547. [CrossRef]

40. Lasko, K. Gap Filling Cloudy Sentinel-2 NDVI and NDWI Pixels with Multi-Frequency Denoised C-Band and L-Band Synthetic Aperture Radar (SAR), Texture, and Shallow Learning Techniques. *Remote Sens.* **2022**, *14*, 4221. [CrossRef]

41. Gessner, U.; Reinermann, S.; Asam, S.; Kuenzer, C. Vegetation Stress Monitor—Assessment of Drought and Temperature-Related Effects on Vegetation in Germany Analyzing MODIS Time Series over 23 Years. *Remote Sens.* **2023**, *15*, 5428. [CrossRef]

42. Colton Flynn, K.; Lee, T.; Endale, D.; Franzluebbers, A.; Ma, S.; Zhou, Y. Assessing Remote Sensing Vegetation Index Sensitivities for Tall Fescue (*Schedonorus arundinaceus*) Plant Health with Varying Endophyte and Fertilizer Types: A Case for Improving Poultry Manuresheds. *Remote Sens.* **2021**, *13*, 521. [CrossRef]

43. Holz, M.; Zarebanadkouki, M.; Benard, P.; Hoffmann, M.; Dubbert, M. Root and Rhizosphere Traits for Enhanced Water and Nutrients Uptake Efficiency in Dynamic Environments. *Front. Plant Sci.* **2024**, *15*, 1383373. [CrossRef]

44. Carminati, A.; Zarebanadkouki, M.; Kroener, E.; Ahmed, M.A.; Holz, M. Biophysical Rhizosphere Processes Affecting Root Water Uptake. *Ann. Bot.* **2016**, *118*, 561–571. [CrossRef] [PubMed]

45. Sahaar, S.A.; Niemann, J.D. Estimating Rootzone Soil Moisture by Fusing Multiple Remote Sensing Products with Machine Learning. *Remote Sens.* **2024**, *16*, 3699. [CrossRef]

46. Llamas, R.M.; Guevara, M.; Rorabaugh, D.; Taufer, M.; Vargas, R. Spatial Gap-Filling of ESA CCI Satellite-Derived Soil Moisture Based on Geostatistical Techniques and Multiple Regression. *Remote Sens.* **2020**, *12*, 665. [CrossRef]

47. Wang, P.; Zeng, J.; Chen, K.S.; Ma, H.; Zhang, X.; Shi, P.; Peng, C.; Bi, H. Global-Scale Assessment of Multiple Recently Developed/Reprocessed Remotely Sensed Soil Moisture Datasets. *IEEE Trans. Geosci. Remote Sens.* **2024**, *62*, 4403518. [CrossRef]

48. Yu, T.; Jiapaer, G.; Bao, A.; Zhang, J.; Tu, H.; Chen, B.; De Maeyer, P.; Van de Voorde, T. Evaluating Surface Soil Moisture Characteristics and the Performance of Remote Sensing and Analytical Products in Central Asia. *J. Hydrol.* **2023**, *617*, 128921. [CrossRef]

49. Muñoz-Sabater, J.; Dutra, E.; Agustí-Panareda, A.; Albergel, C.; Arduini, G.; Balsamo, G.; Boussetta, S.; Choulga, M.; Harrigan, S.; Hersbach, H.; et al. ERA5-Land: A State-of-the-Art Global Reanalysis Dataset for Land Applications. *Earth Syst. Sci. Data* **2021**, *13*, 4349–4383. [CrossRef]

50. Hersbach, H.; Bell, B.; Berrisford, P.; Hirahara, S.; Horányi, A.; Muñoz-Sabater, J.; Nicolas, J.; Peubey, C.; Radu, R.; Schepers, D.; et al. The ERA5 Global Reanalysis. *Q. J. R. Meteorol. Soc.* **2020**, *146*, 1999–2049. [CrossRef]

51. Siles, G. ERA5 Climatic Reanalysis: A Review on Its Use for Calculating Atmospheric Attenuation for Satellite Communication Systems. *Rev. Investig. Desarro.* **2022**, *22*, 145–159. [CrossRef]

52. Tahmouresi, M.S.; Niksokhan, M.H.; Ehsani, A.H. Enhancing Spatial Resolution of Satellite Soil Moisture Data through Stacking Ensemble Learning Techniques. *Sci. Rep.* **2024**, *14*, 25454. [CrossRef]

53. Bueno, M.; García, C.B.; Montoya, N.; Rau, P.; Loayza, H. Watershed Scale Soil Moisture Estimation Model Using Machine Learning and Remote Sensing in a Data-Scarce Context. *Sci. Agropecu.* **2024**, *15*, 103–120. [CrossRef]

54. Xiao, C.; Wu, Y.; Zhu, X. Evaluation of the Monitoring Capability of 20 Vegetation Indices and 5 Mainstream Satellite Band Settings for Drought in Spring Wheat Using a Simulation Method. *Remote Sens.* **2023**, *15*, 4838. [CrossRef]

55. Govedar, Z.; Anikić, N. Vegetation Indices Monitoring by Using Copernicus Data in the Old-Growth Forests of the Republic of Srpska/Bosnia and Herzegovina. *Front. For. Glob. Change* **2024**, *7*, 1354769. [CrossRef]

56. Yang, H.; Yang, X.; Heskel, M.; Sun, S.; Tang, J. Seasonal Variations of Leaf and Canopy Properties Tracked by Ground-Based NDVI Imagery in a Temperate Forest. *Sci. Rep.* **2017**, *7*, 1267. [CrossRef]

57. Huang, X.; Zhang, T.; Yi, G.; He, D.; Zhou, X.; Li, J.; Bie, X.; Miao, J. Dynamic Changes of Ndvi in the Growing Season of the Tibetan Plateau during the Past 17 Years and Its Response to Climate Change. *Int. J. Environ. Res. Public Health* **2019**, *16*, 3452. [CrossRef]

58. Longchamps, L.; Philpot, W. Full-Season Crop Phenology Monitoring Using Two-Dimensional Normalized Difference Pairs. *Remote Sens.* **2023**, *15*, 5565. [CrossRef]

59. Gim, H.J.; Ho, C.H.; Jeong, S.; Kim, J.; Feng, S.; Hayes, M.J. Improved Mapping and Change Detection of the Start of the Crop Growing Season in the US Corn Belt from Long-Term AVHRR NDVI. *Agric. For. Meteorol.* **2020**, *294*, 108143. [CrossRef]

60. Olmos-Trujillo, E.; González-Trinidad, J.; Júnez-Ferreira, H.; Pacheco-Guerrero, A.; Bautista-Capetillo, C.; Avila-Sandoval, C.; Galván-Tejada, E. Spatio-Temporal Response of Vegetation Indices to Rainfall and Temperature in a Semiarid Region. *Sustainability* **2020**, *12*, 1939. [CrossRef]

61. Marusig, D.; Petruzzellis, F.; Tomasella, M.; Napolitano, R.; Altobelli, A.; Nardini, A. Correlation of Field-Measured and Remotely Sensed Plant Water Status as a Tool to Monitor the Risk of Drought-Induced Forest Decline. *Forests* **2020**, *11*, 77. [CrossRef]

62. Shashikant, V.; Shariff, A.R.M.; Wayayok, A.; Kamal, R.; Lee, Y.P.; Takeuchi, W. Utilizing TVDI and NDWI to Classify Severity of Agricultural Drought in Chuping, Malaysia. *Agronomy* **2021**, *11*, 1243. [CrossRef]

63. Pôças, I.; Calera, A.; Campos, I.; Cunha, M. Remote Sensing for Estimating and Mapping Single and Basal Crop Coeficientes: A Review on Spectral Vegetation Indices Approaches. *Agric. Water Manag.* **2020**, *233*, 106081. [CrossRef]

64. Abbasi, N.; Nouri, H.; Didan, K.; Barreto-Muñoz, A.; Chavoshi Borujeni, S.; Opp, C.; Nagler, P.; Thenkabail, P.S.; Siebert, S. Mapping Vegetation Index-Derived Actual Evapotranspiration across Croplands Using the Google Earth Engine Platform. *Remote Sens.* **2023**, *15*, 1017. [CrossRef]

65. Niu, H.; Wang, D.; Chen, Y. Estimating Crop Coefficients Using Linear and Deep Stochastic Configuration Networks Models and UAV-Based Normalized Difference Vegetation Index (NDVI). In Proceedings of the 2020 International Conference on Unmanned Aircraft Systems (ICUAS), Athens, Greece, 1–4 September 2020; pp. 1485–1490.

66. Stone, K.C.; Bauer, P.J.; Sigua, G.C. Managing Variable-Rate Irrigation Using NDVI. In Proceedings of the 14th International Conference on Precision Agriculture, Montreal, QC, Canada, 24–27 June 2016.

67. Elagib, N.A.; Musa, A.A. Correcting Hargreaves-Samani Formula Using Geographical Coordinates and Rainfall over Different Timescales. *Hydrol. Process.* **2023**, *37*, e14790. [CrossRef]

68. Gourgouletis, N.; Gkavrou, M.; Baltas, E. Comparison of Empirical ETo Relationships with ERA5-Land and In Situ Data in Greece. *Geographies* **2023**, *3*, 499–521. [CrossRef]

69. Wu, Z.; Chen, X.; Cui, N.; Zhu, B.; Gong, D.; Han, L.; Xing, L.; Zhen, S.; Li, Q.; Liu, Q.; et al. Optimized Empirical Model Based on Whale Optimization Algorithm for Simulate Daily Reference Crop Evapotranspiration in Different Climatic Regions of China. *J. Hydrol.* **2022**, *612*, 128084. [CrossRef]